

Licochalcone A induces cell cycle arrest and apoptosis via suppressing MAPK signaling pathway and the expression of FBXO5 in lung squamous cell cancer

XIAOLI FAN¹, GUOQIANG GUAN², JUAN WANG², MEIHUA JIN³, LIMING WANG³ and XIAOQUN DUAN⁴

¹Department of Pharmacy, Xiangya Hospital, Central South University, Changsha, Hunan 410013;

²College of Pharmacy, Guilin Medical University, Guilin, Guangxi 541199; ³Affiliated Hospital of

Guilin Medical University, Guilin, Guangxi 541001; ⁴Industrial Technology Research

Institute of Pharmacy, Guilin Medical University, Guilin, Guangxi 541199, P.R. China

Received June 13, 2023; Accepted October 2, 2023

DOI: 10.3892/or.2023.8651

Abstract. Lung squamous cell carcinoma (LSCC) is a highly heterogeneous malignancy with high mortality and few therapeutic options. Licochalcone A (LCA, PubChem ID: 5318998) is a chalcone extracted from licorice and possesses anticancer and anti-inflammatory activities. The present study aimed to elucidate the anticancer effect of LCA on LSCC and explore the conceivable molecular mechanism. MTT assay revealed that LCA significantly inhibited the proliferation of LSCC cells with less cytotoxicity towards human bronchial epithelial cells. 5-ethynyl-2'-deoxyuridine (EdU) assay demonstrated that LCA could reduce the proliferation rate of LSCC cells. The flow cytometric assays indicated that LCA increased the cell number of the G1 phase and induced the apoptosis of LSCC cells. LCA downregulated the protein expression of cyclin D1, cyclin E, CDK2 and CDK4. Meanwhile, LCA increased the expression level of Bax, cleaved poly(ADP-ribose)polymerase-1 (PARP1) and caspase 3, as well as downregulated

the level of Bcl-2. Proteomics assay demonstrated that LCA exerted its antitumor effects via inhibiting mitogen-activated protein kinase (MAPK) signaling pathways and the expression of F-box protein 5 (FBXO5). Western blot analysis showed that LCA decreased the expression of p-ERK1/2, p-p38MAPK and FBXO5. In the xenograft tumors of LSCC, LCA significantly inhibited the volumes and weight of tumors in nude mice with little toxicity in vital organs. Therefore, the present study demonstrated that LCA effectively inhibited cell proliferation and induced apoptosis *in vitro*, and suppressed xenograft tumor growth *in vivo*. LCA may serve as a future therapeutic candidate of LSCC.

Introduction

Lung cancer is the leading cause of cancer-related death in the world, followed by colorectal, liver and stomach cancers (1,2), and non-small cell lung cancer (NSCLC) accounts for ~85% of patients with lung cancer (3,4). Lung squamous cell carcinoma (LSCC) is the second most common histological subtype and is associated with poor prognosis (5). Despite the diagnosis and treatment of NSCLC have been advanced, the main treatment strategy for LSCC remains surgical resection or radiation with chemotherapy (6,7). However, the recurrence rate was high among the patients who suffer postoperative (8). Previously, PD1/PD-L1 immunotherapies have improved the clinical outcome of patients with NSCLC and demonstrated a notable efficacy (9-11), and targeted therapies have improved outcomes for certain subtypes, but patients with LSCC are not likely to benefit from these treatments (12). Thus, it is imperative to search for new drugs and effective therapeutic strategies against LSCC to reduce the mortality rate.

Nowadays, numerous natural medicines have been proved to inhibit or reverse the progression of several cancers and appeared to be promising novel anticancer drugs due to high efficiency and low toxicity. Licochalcone A (LCA) is a natural and useful flavonoid extracted from licorice, which possesses several pharmacological properties such as antibacterial (13), antitumor (14), anti-inflammatory (15,16) and antioxidation properties (17). In recent decades, studies have demonstrated

Correspondence to: Mr. Liming Wang, Affiliated Hospital of Guilin Medical University, 15 Lequn Road, Xiufeng, Guilin, Guangxi 541001, P.R. China

E-mail: wlmkeyan@126.com

Professor Xiaoqun Duan, Industrial Technology Research Institute of Pharmacy, Guilin Medical University, 1 Zhiyuan Road, Lingui, Guilin, Guangxi 541199, P.R. China

E-mail: robertduan@163.com

Abbreviations: LSCC, lung squamous cell carcinoma; LCA, licochalcone A; FCM, flow cytometry; 4D-DIA proteomics, 4D-data-independent acquisition proteomics; MAPK, mitogen-activated protein kinase; ERK1/2, extracellular regulated protein kinases 1 and 2; CDK2, cyclin dependent kinase 2; CDK4, cyclin dependent kinase 4; PARP1, poly(ADP-ribose)polymerase-1; FBXO5, F-box protein 5

Key words: licochalcone A, lung squamous cell carcinoma, apoptosis, proteomics, F-box protein 5

that LCA exhibited potent antitumor effects in several epithelial carcinoma cells by regulating numerous signaling pathways, such as the oxidative stress, the mitogen-activated protein kinase (MAPK) and the apoptosis pathway (18). For example, LCA induced apoptosis of gastric cancer cells by activating the MAPK and PI3K/AKT signaling pathways (17). However, LSCC is a distinct subtype of NSCLC, and the antitumor effects of LCA on LSCC remain unknown.

F-box protein 5 (FBXO5) is involved in the regulation of proliferation, apoptosis, epithelial-mesenchymal transition and drug resistance (19,20). FBXO5 promotes proper mitotic entry by blocking the anaphase-promoting complex/cyclosome activity (21,22). It functions as a cell cycle regulator and plays a crucial role in proliferation and tumorigenesis (23,24). Evidence indicates that FBXO5 is upregulated in various malignant tumors compared with matched normal tissues. Previous research indicated that high FBXO5 expression would cause genomic instability and mitotic catastrophe, contributing to tumorigenesis of breast cancer (25) and esophageal squamous cell carcinoma (26). In addition, existing evidence has suggested that FBXO5 expression level was higher in LSCC compared with normal tissue, and the overexpressed FBXO5 leads to shorter overall survival (OS) in patients with LSCC (27). Therefore, FBXO5 may be a potential oncogene and therapeutic target in LSCC.

The present study aimed to detect the effect of LCA on cell proliferation, cell cycle, apoptosis and gene expression on LSCC *in vitro* and the antitumor activities *in vivo*, and further explore the underlying mechanisms.

Materials and methods

Cell culture. The LSCC cells H226 (cat. no. TCHu235), H1703 (cat. no. SCSP-593) and human bronchial epithelial cells (HBE; cat. no. CL-0346) were maintained in RPMI-1640 (cat. no. C11875500BT) media supplemented with 10% fetal bovine serum (cat. no. 10099-141C; Gibco; Thermo Fisher Scientific, Inc.) and cultured in a 37°C incubator set with 5% CO₂, humidified environment. H226 and H1703 cells were purchased from The Cell Bank of Type Culture Collection of The Chinese Academy of Sciences. HBE cells were purchased from Procell Life Science & Technology Co., Ltd.

Chemical reagents and antibodies. LCA (Cas. no. 58749-22-7; Fig. 1A; cat. no. S01015) was purchased from Nanjing Dilger Medical Technology Co. Ltd. and dissolved in dimethyl sulfoxide (DMSO; cat. no. D8371; Beijing Solarbio Science & Technology Co., Ltd.). FITC Annexin V Apoptosis Detection kit was acquired from BD (cat. no. 556547, BD Pharmingen; BD Biosciences). CDK2 (1:1,000; cat. no. ab32147; Abcam), CDK4 (1:1,000; cat. no. ab108357; Abcam), cyclin D1 (1:5,000; cat. no. ab134175; Abcam), cyclin E (1:1,000; cat. no. WL01072; Wanleibio Co., Ltd.), cleaved caspase 3 (1:1,000; cat. no. AF7022; Affinity Biosciences, Ltd.), cleaved poly(ADP-ribose)polymerase-1 (PARP1) (1:5,000; cat. no. ab32064; Abcam), ERK (1:1,000; cat. no. ab184699; Abcam), phosphorylated (p)-JERK (1:1,000; cat. no. ab201015; Abcam), p38 MAPK (1:1,000; cat. no. 8690; Cell Signaling Technology, Inc.), p-p38 MAPK (1:1,000; cat. no. 4511; Cell Signaling Technology, Inc.), FBXO5 (1:5,000; cat. no. ab184950; Abcam),

GAPDH (1:5,000; cat. no. 60004-1-IG; Proteintech Group, Inc.), HRP-goat anti-mouse (1:5,000; cat. no. EM35110-01; Beijing Emarbio Science & Technology Co., Ltd.) and HRP-goat anti-rabbit antibody (1:5,000; cat. no. EM35111-01; Beijing Emarbio Science & Technology Co., Ltd.).

MTT detection. The cells were seeded in 96-well plates at a density of 5x10³ cells per well in a 100-μl medium and incubated overnight. The H226 and H1703 cells were cultured with LCA at a dose of 0, 2, 5, 10, 20 and 40 μM for 24, 48 and 72 h. HBE cells were cultured in the medium with a concentration of 0, 10, 20, 40, 60 and 80 μM LCA for 24 and 48 h. After treatment, 20 μl of 5 mg/ml MTT (Beijing Solarbio Science & Technology Co., Ltd.) was added to the well and incubated for at least 3 h in an incubator set at 37°C, then the medium was removed from each well and 200 μl DMSO was added. The absorbance at the wavelength of 490 nm (OD value) was measured by Infinite M200 Pro NanoQuant (Tecan Group, Ltd.) and then the cell viability and IC₅₀ value were measured according to the OD value. Based on the result of MTT, the IC₅₀ was calculated for H226 and H1703 cells. Subsequently, LCA was selected at the dose of 0, 10, 20 and 40 μM in the following experiments.

5-ethynyl-2'-deoxyuridine (EdU) staining. Cell proliferation was detected using BeyoClick™ EdU-488 Assay kit (cat. no. C0071S; Beyotime Institute of Biotechnology). LSCC cells were plated in six-well plates and incubated overnight, then treated with different doses of LCA for 16 h. EdU solution was prepared and final 10 μM EdU working solution was added to the medium for incubating for 3 h at 37°C. Subsequently, 4% paraformaldehyde was used to fix cells for 15 min and washed off with PBS containing 3% BSA (Beijing Solarbio Science & Technology Co., Ltd.). Next, the cells were permeabilized with enhanced immunostaining permeabilization buffer (cat. no. P0097; Beyotime Institute of Biotechnology) for 15 min and washed. Then, the EdU detection was performed followed the manufacturer's protocols and the nuclei were stained with Hoechst 33342 for 10 min while avoiding light at room temperature. Fluorescence images were obtained by Olympus microscope (Olympus Corporation). The number of EdU-positive cells was counted and calculated in five randomly selected fields. Cell proliferation rate=EdU-positive cells/DAPI-positive cells x100%. The experiments were performed in triplicate.

Cell cycle assay. The cell cycle distribution was evaluated by FCM using propidium iodide (PI; cat. no. P8080; Beijing Solarbio Science & Technology Co., Ltd.). H226 and H1703 cells were cultured in 6 cm dishes and treated with LCA (0, 10, 20 and 40 μM) for 24 h in a 37°C incubator set with 5% CO₂, humidified environment. After treatment, the cells were harvested and resuspended, and subsequently fixed with 70% cold ethyl alcohol overnight at 4°C. The next day, cells were centrifuged at 1,000 x g for 10 min and washed. Following this, the cells were incubated with RNase A and 500 μl PI in a 37°C water bath for 30 min. The cell cycle distribution of LSCC was measured on the Accuri C6 flow cytometer (BD Biosciences) and analyzed with FlowJo 7.6 software (FlowJo LLC).

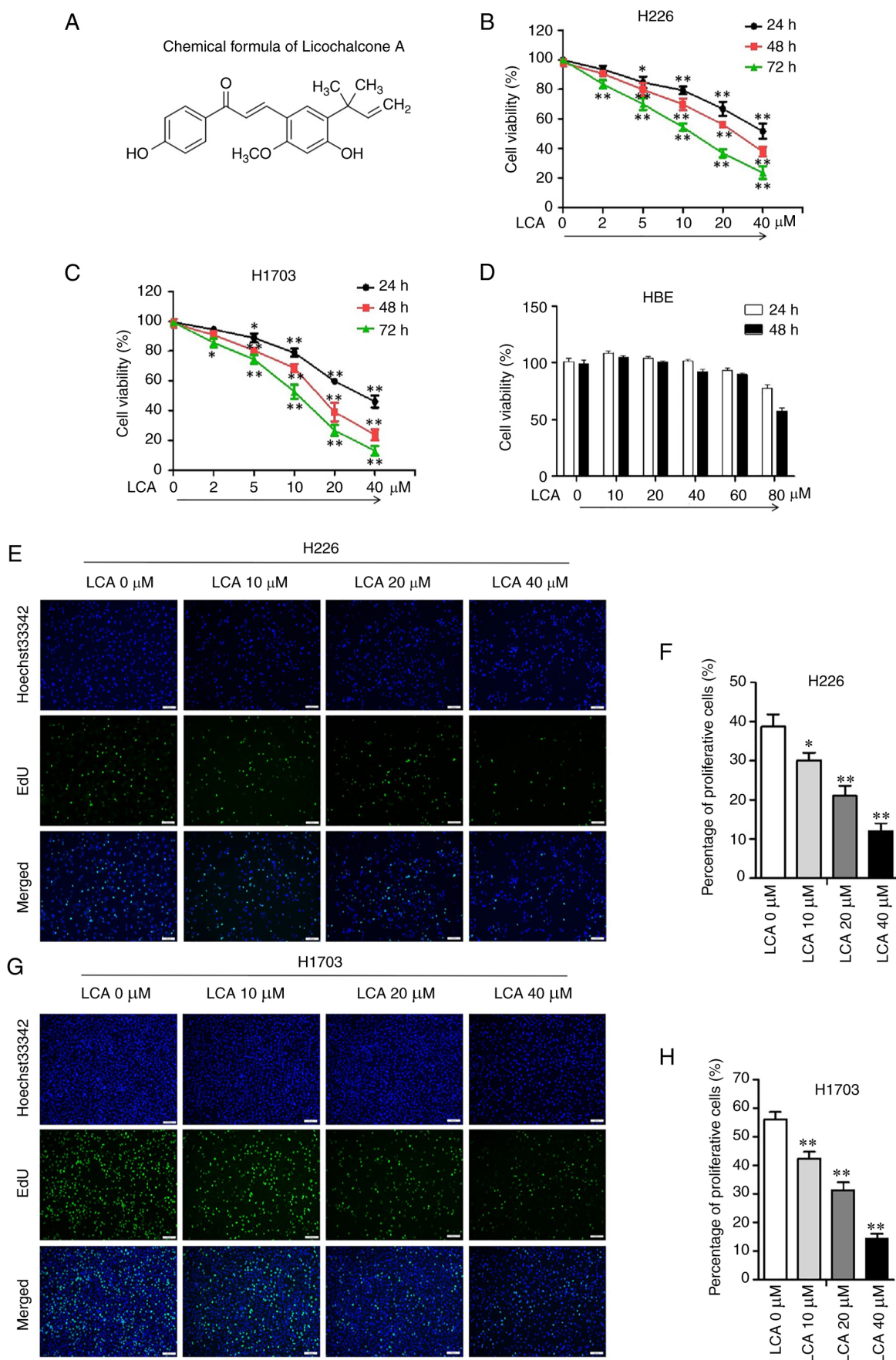


Figure 1. LCA inhibits lung squamous cell carcinoma cell viability and proliferation. (A) Chemical structure of LCA. (B and C) The viability of H226 and H1703 cells after treatment with LCA was detected by MTT. (D) The viability of HBE cells after treatment with LCA was detected by MTT. (E and F) EdU staining assay was used to detect cell proliferative ability of H226 cells (scale bar, 200 μm). (G and H) EdU staining assay was used to detect cell proliferative ability of H1703 cells (scale bar, 200 μm). The experiments were repeated at least three times (n=3). *P<0.05 and **P<0.01 vs. 0 μM. LCA, licochalcone A; EdU, 5-ethynyl-2'-deoxyuridine.

Cell apoptosis assay. Cellular apoptosis was evaluated by FCM using FITC-Annexin V Apoptosis Detection Kit. H226 and H1703 cells were treated with LCA (0, 10, 20 and 40 μM) for 24 h in a 37°C incubator set with 5% CO_2 , humidified environment. After treatment, the cells were harvested and assayed according to the manufacturer's instructions. The apoptotic rate was analyzed by the Accuri C6 flow cytometer (BD Biosciences).

4D-data-independent acquisition (4D-DIA) proteomics. H1703 cells were cultured overnight in 100-mm culture dishes until the density reached 40-50%. Subsequently, the cells were treated with or without 40 μM LCA for 24 h in a 37°C incubator set with 5% CO_2 , humidified environment. The medium was aspirated, and the cells were washed with pre-cooled PBS solution twice. Next, the cells were gently scraped off with cell scraper and transferred to a centrifuge tube, centrifuged at 4°C, 300-500 \times g for 5 min, the supernatant was discarded and washed once with PBS. PBS was added to make cell suspensions and 1×10^7 cells were counted in each sample by a cell counter. The cells were immediately frozen with liquid nitrogen for 5-10 min, then stored in a -80°C refrigerator for proteomics assay. Before the differential protein expression assays, the qualitative and quantitative protein analysis of the 4D mass spectrometry data was performed by DIA-NN (v1.8.1) software. The Pearson's correlation analysis was used to evaluate the correlation among samples. Principal component analysis (PCA) was used to understand the variances between the different sample groups.

Network pharmacological analysis. PubChem (<https://pubchem.ncbi.nlm.nih.gov/>) was used for searching 'LCA' and obtained the SMILES number, the potential targets genes of LCA were predicted by SwissTarget Prediction (<http://www.swisstargetprediction.ch/>). The potential LSCC therapeutic targets were identified by DisGeNET databases (<https://www.disgenet.org/search>). The Sangerbox (<http://sangerbox.com/>) was used to perform the Gene Ontology and Kyoto Encyclopedia of Genes and Genomes (KEGG) pathway enrichment analyses of the differentially expressed genes (DEGs). The DEGs were imported into the Venny 2.1 online tool (<https://bioinfogp.cnb.csic.es/tools/venny/index.html>) to screen the overlapping genes. Protein-protein interaction (PPI) analysis was performed using the STRINGDB (<http://string-db.org/>) protein interaction database.

Bioinformatics analyses. The TIMER2.0 database (<http://timer.cistrome.org/>) and UALCAN database (<https://ualcan.path.uab.edu/analysis>) were used to study the DEGs between tumor and adjacent normal tissues based on The Cancer Genome Atlas (TCGA) project. In TIMER 2.0 database, the differential expression between tumor and adjacent normal tissues for any gene of interest across all TCGA tumors. Distributions of gene expression levels are displayed using box plots. The statistical significance computed by the Wilcoxon test is annotated by the number of stars (* $P < 0.05$, ** $P < 0.01$ and *** $P < 0.001$).

Molecular docking. The canonical 2D structure of Licochalcone A (CAS no. 58749-22-7) was obtained from PubChem (<https://pubchem.ncbi.nlm.nih.gov/>). ChemOffice

software (<https://www.downza.cn/>) was used to optimize and minimize the structure energy of LCA, then convert the 2D structure to 3D. The ID of FBXO5 (Q9UKT4) was obtained from Uniprot database (<https://www.uniprot.org/>), and the crystal structure of the FBXO5 (PDB ID: 2M6N) was obtained from PDB database (<http://www.rcsb.org/>). The mol2 files of LCA and the PDB files of FBXO5 were imported to AutoDock Tools, converted to PDBQT format and parameters were set to determine the active pocket. Molecular docking was performed with AutoDock 1.5.6 software. The docking image was acquired using PyMol software (<https://pymol.org/2/>).

Transient transfection of small interfering siRNA. siRNAs against FBXO5 (si-FBXO5) and the negative control siRNA (si-NC) were purchased from CENTRAL BIOL (www.generalbiol.com/). The sequences of si-FBXO5 and si-NC are listed in Table SI. H1703 cells were transfected with si-FBXO5 and si-NC for 24 h at 37°C using Lipofectamine® 3000 (cat no. L3000-015; Invitrogen; Thermo Fisher Scientific, Inc.) according to the manufacturer's instructions. The concentration of siRNAs used in the present study was 50 nM. Subsequent experiments were performed 24 h after siRNA transfection.

In vivo xenograft experiment. All operation procedures of this animal study were approved by the Institutional Animal Care and Use Committee of Guilin Medical University (approval no. GLMC-IACUC-2021016; Guilin, China). A total of 20 BALB/c-nu mice (male) at the age of 4 weeks (mean weight, 16 ± 0.5 g) were obtained from Hunan SJA Laboratory Animal Co., Ltd. The mice were housed in pathogen-free environment with controlled temperature (20-25°C), humidity (40-70%), and free access to rodent chow and water. After 5 days of acclimation, equal volumes (200 μl) of 4×10^6 H1703 cells resuspended in PBS (4×10^6 cells/mouse) were injected into the right flank of mice. After 7 days, when the tumors were visible, the mice were divided into 4 groups randomly ($n=5$): i) The control group (saline containing 20% SBE- β -CD), ii) the LCA 7.5 mg/kg group, iii) the LCA 15 mg/kg group and iv) the cisplatin (CDDP) 2 mg/kg group. LCA was dissolved in saline containing 20% SBE- β -CD. The mice were intraperitoneally injected with 200 μl of drugs once a day for 10 days. The body weight, length and width of the tumor were measured every day, and the tumor volume was calculated as follows: length \times width²/2. During the process of the animal experiments, none of the mice succumbed. After 10 days of LCA administration, the mice were anesthetized by intraperitoneal injection of sodium pentobarbital (50 mg/kg) and euthanized by cervical dislocation. The humane endpoints included the tumor volume in the control group (if it reached $\sim 1,500$ mm³) and the dietary activities (if they were interfered). The tumors and vital organs were excised and weighted after the absence of a heartbeat and breath, one portion of the tumor was frozen with liquid nitrogen immediately for western blotting, while the other portion was fixed in paraformaldehyde for histopathological experiments. The vital organs (heart, liver, spleen, lung and kidney) were fixed in paraformaldehyde for hematoxylin and eosin (H&E) staining.

Western blot analysis. LSCC cells treated with LCA at the concentration of 0, 10, 20 and 40 μM . After treatment, the cells were harvested and lysed in cold RIPA lysis buffer (cat. no. P0013B; Beyotime Institute of Biotechnology) with PMSF and protease inhibitor for 30 min on ice. The supernatant was collected after being centrifuged and the concentration was measured by BCA kit (Beyotime Biotechnology). A total of 20 μg of protein was separated by SDS-PAGE (10-12%) electrophoresis and further transferred onto the nitrocellulose membrane. Subsequently, the membrane was blocked with 5% non-fat milk in TBST buffer at room temperature for 2 h and was then incubated overnight under the primary antibodies at 4°C. After washed for 3 times with TBST, the membrane was incubated with secondary antibody for 1 h at room temperature the next day. The specific bands were visualized by ECL kit (cat. no. P0018S; Beyotime Institute of Biotechnology) and analyzed by ImageJ (v1.48) software (National Institutes of Health).

Histopathology. Tumor tissues and vital organs were fixed in paraformaldehyde (4% PFA) for 24 h at room temperature. A serial alcohol gradient was used to dehydrate the tissues, after dehydration, the tissues were embedded on paraffin wax blocks. The paraffin blocks were cut to 4- μm sections for H&E staining (hematoxylin for 5 min and eosin for 3 min) at room temperature. Images were captured using a light microscope (Olympus Corporation).

Statistical analysis. All data were performed using the GraphPad Prism 5 (Dotmatics) and SPSS software version 23.0 (IBM Corp.). The paired Student's t-test was used on data between two groups after testing for normality and homogeneity of variance, and one-way ANOVA was used for multiple comparisons followed by the post hoc Bonferroni test. The data was expressed as the mean \pm standard deviation (SD), and $P < 0.05$ was considered to indicate a statistically significant difference.

Results

LCA inhibits the proliferation in LSCC cells but not in HBE cells in vitro. MTT assay revealed that LCA significantly inhibited the cell viability in H226 (Fig. 1B) and H1703 (Fig. 1C) cells. Furthermore, the inhibitory effect of LCA (5, 10, 20 and 40 μM) on LSCC cells was in a dose and time-dependent manner. The MTT result showed that the cell viability of HBE was 93.31 ± 2.98 and $89.66 \pm 2.25\%$ when the concentration of LCA was 60 μM at 24 and 48 h (Fig. 1D). These results indicated that LCA exhibited no significant cytotoxicity against HBE cells in a treatment with up to 60 μM of the drug. EdU staining assay indicated that the proliferation rate was significantly reduced in H226 (Fig. 1E and F) and H1703 cells (Fig. 1G and H) after LCA treatment. These results revealed that LCA suppressed the proliferation capacity of LSCC cells.

LCA induces cell cycle arrest in LSCC cells. To assess the effect of LCA on cell cycle, the distribution of cell cycle in H226 and H1703 cells after treatment with different concentrations of LCA was investigated by FCM. As illustrated

in Fig. 2A and B, the proportion of G1 phase at concentrations of 0, 10, 20 and 40 μM in H226 cells were 43.70 ± 0.78 , 48.40 ± 2.03 , 54.67 ± 2.71 and $61.33 \pm 2.19\%$, respectively, and the ratio of cells at G2 phase was decreased. LCA significantly induced G1 phase arrest in a dose-dependent manner (10, 20 or 40 vs. control: $P < 0.05$, $P < 0.01$ or $P < 0.01$) in H226 cells. Similarly, in H1703 cells, the G1 phase proportion at concentrations of 0, 10, 20 and 40 μM were 52.03 ± 6.09 , 61.93 ± 5.92 , 73.47 ± 9.07 and $83.40 \pm 3.15\%$, respectively, and the ratio of cells at S phase decreased. LCA at concentrations of 20 and 40 μM could significantly increase the G1 phase proportion (20 or 40 vs. control: $P < 0.01$ or $P < 0.01$) in H1703 cells. These results indicated that LCA treatment significantly increased the distribution of G1 phase in a dose-dependent manner in a certain range of concentrations. According to the results, the expression level of proteins related to G1 phase was further explored. Western blot analysis results (Fig. 2C and D) indicated that LCA decreased the protein levels of cyclin D1, cyclin E, CDK2 and CDK4 in H226 cells and H1703 cells. These results suggested that LCA caused G1 phase arrest by regulating the proteins related to G1 phase.

LCA induces apoptosis in LSCC cells. The cell apoptosis of LSCC induced by LCA were performed through FCM with the annexin V/PI double staining method. After LCA treated for 24 h, the apoptotic rates of H226 cells at concentrations of 0, 10, 20, and 40 μM were 6.13 ± 1.16 , 7.67 ± 1.37 , 14.07 ± 1.70 and $28.20 \pm 2.47\%$, respectively. Similarly, in H1703 cells, the apoptotic rates were 5.03 ± 0.64 , 8.37 ± 0.95 , 14.17 ± 3.65 and $21.93 \pm 3.35\%$, respectively (Fig. 3A and B). At the concentration of 20 and 40 μM , the apoptotic rates were significantly increased in both H226 and H1703 cells compared with control ($P < 0.01$). These results demonstrated that LCA could induce apoptosis in dose-dependent manner within the range of certain concentrations. As demonstrated in Fig. 3C and D, western blot analysis results indicated that LCA significantly increased the expression level of Bax, cleaved PARP1 and cleaved caspase 3 in H226 and H1703 cells, while decreased the level of Bcl-2. Overall, these results indicated that LCA induced cell apoptosis by the mitochondrial-mediated pathway in LSCC cells.

Proteomic analysis. 4D-DIA quantitative proteomic technique was used to identify the differential proteins and potential molecular mechanisms after LCA treatment in LSCC cells. Most of the peptides were distributed at 7-20 amino acids and the distribution of peptide length met the quality control requirements (Fig. 4A). Box plots and violin plots (Fig. 4B) indicated favorable consistency within the sample group. Pearson's correlation coefficients indicated high correlation in the expression patterns between the samples (Fig. 4C). PCA revealed satisfactory repeatability in the samples of control and LCA treatment group (Fig. 4D). Histogram (Fig. 4E) and Volcano plots (Fig. 4F) demonstrated a total of 1101 differentially expressed proteins (DEPs) after LCA treated, including 616 upregulated and 485 downregulated DEPs. The heatmap revealed the clustering of DEGs between the control and LCA-treatment group (Fig. 4G). Enrichment analyses of these DEPs based on KEGG databases revealed that PI3K/Akt signaling pathway, AMPK signaling pathway, Hippo signaling

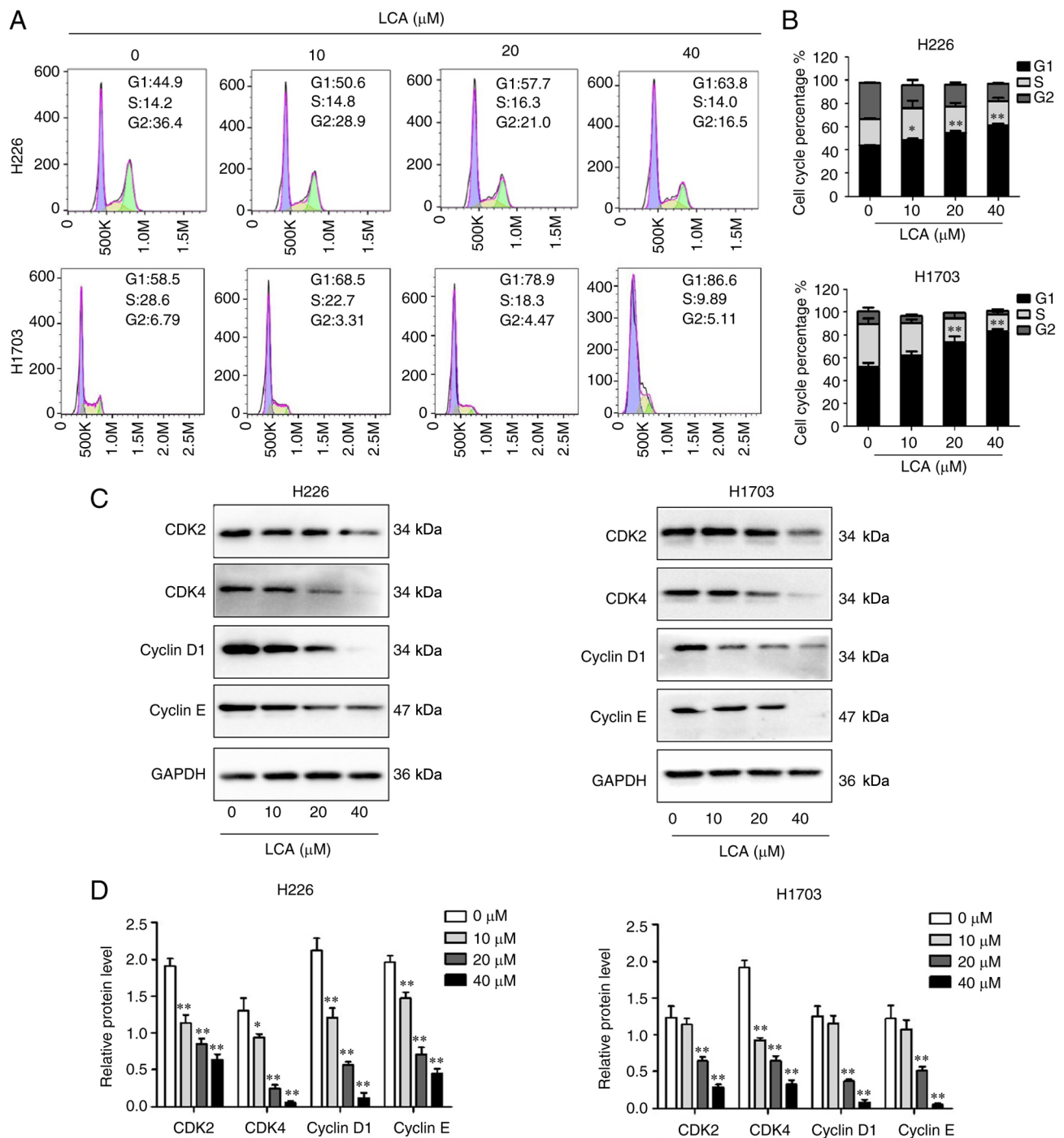


Figure 2. The effect of LCA on cell cycle in lung squamous cell carcinoma cells. (A and B) Analysis of the cell cycle proportion of H226 and H1703 cells after treated with LCA (0, 10, 20 and 40 μM) by flow cytometry. (C and D) The protein expression of CDK2, CDK4, cyclin D1 and cyclin E in H226 and H1703 cells determined by western blot analysis after treatment with LCA. The intensity of the bands was quantified by ImageJ and GAPDH was used as control. The experiments were repeated at least three times ($n=3$). * $P<0.05$ and ** $P<0.01$ vs. 0 μM . LCA, licochalcone A.

pathway, FoxO signaling pathway and MAPK signaling pathway were enriched (Fig. 4H).

Network pharmacological analysis. The SwissTarget Prediction database search revealed that 101 relevant targets for LCA were obtained. Disgenet databases identified 671 potential therapeutic targets related to LSCC. Comparative analysis of the targets obtained 17 overlapping genes (Fig. 5A). Moreover, the KEGG Pathway enrichment results detected that the DEPs

mainly involved in pathways in cancer, microRNAs in cancer, PI3K/Akt signaling pathway and MAPK signaling pathway (Fig. 5B). These signaling pathways may be closely related to the effects of LCA treatment in LSCC. A PPI network was constructed among the 17 differentially expressed proteins. The interacting proteins were MAPK1 (ERK2), MAPK14 (p38 MAPK), EGFR, PTGS2, PDGFRB, MMP9, MMP14, GLI1, MDM2, HPGDS, ABCB1, RET and THRB (Fig. 5C); and the MAPK1 (ERK2), MAPK14 (p38 MAPK), EGFR,

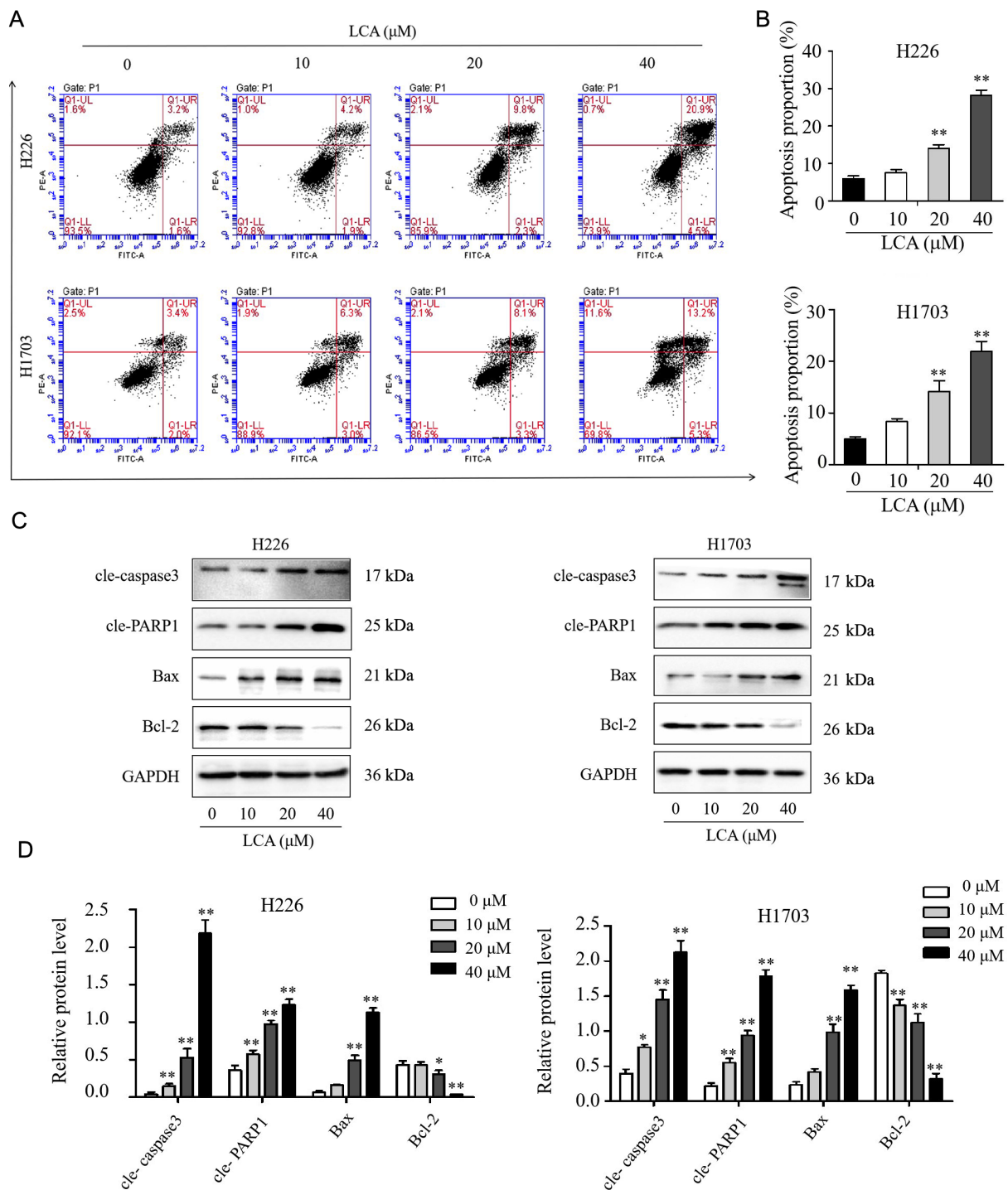


Figure 3. The effect of LCA on cell apoptosis in lung squamous cell carcinoma cells. (A and B) The apoptotic rates of H226 and H1703 cells after treatment with LCA were detected by flow cytometry. (C and D) The level of apoptosis-related proteins of H226 and H1703 cells determined by western blot analysis. The experiments were repeated at least three times (n=3). * $P<0.05$ and ** $P<0.01$ vs. 0 μ M. LCA, licochalcone A; cle-, cleaved; PARP1, poly(ADP-ribose) polymerase-1.

PTGS2, PDGFRB were the core targets. Combined with the results of proteomics, it was hypothesized that LCA inhibits proliferation of LSCC via suppression of the MAPK signaling pathways. Subsequently, western blotting results demonstrated that LCA treatment inhibited the expression of p-p38 MAPK and p-ERK1/2 in a dose-dependent manner while the total p38 MAPK and ERK1/2 were not changed in both H1703 and H226 cells (Fig. 5D-F).

Bioinformatics analysis. The top 5 upregulated and down-regulated DEPs obtained from proteomic analysis were presented in Table I. Bioinformatics analysis of these 10 DEPs through TIMER databases demonstrated that FBXO5 level was higher in 14 types of cancer, such as LIHC, lung adenocarcinoma, LSCC, bladder and breast cancer (Fig. 6A). The FBXO5 expression was significantly elevated in LSCC compared with the corresponding normal tissues through

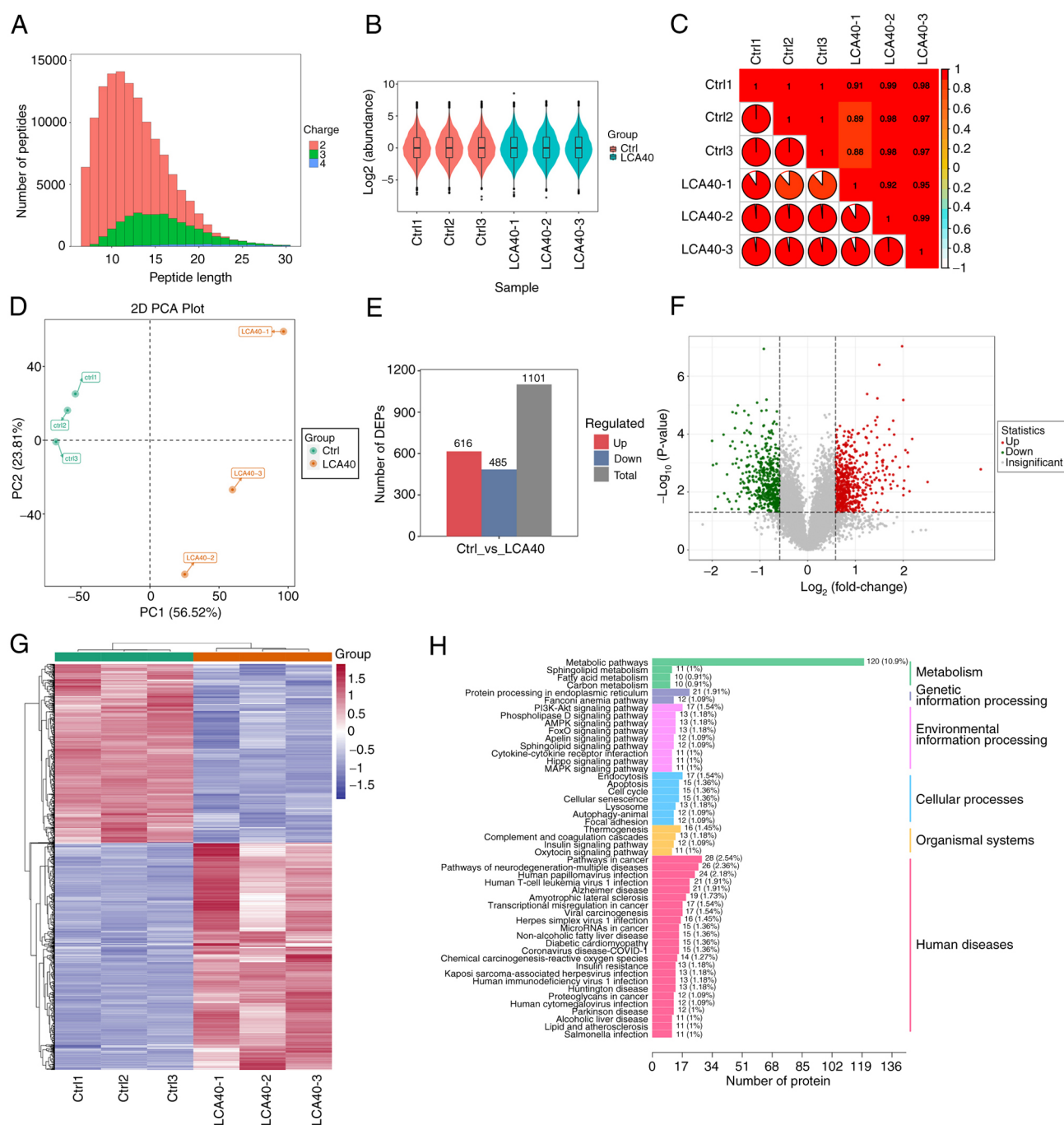


Figure 4. Proteomic analysis of control and the LCA-treated LSCC cells. (A) Distribution of peptide length. (B) Distribution of the sample abundance. (C) Pearson's correlation analysis of the protein expression patterns. (D) Principal component analysis. (E and F) The histogram and volcano plots demonstrated the 1101 DEPs including 616 upregulated and 485 downregulated after LCA treatment in LSCC cells. (G) The heatmap revealed the different expression patterns of the differentially expressed genes. (H) Kyoto Encyclopedia of Genes and Genomes pathway analysis. LCA, licochalcone A; LSCC, lung squamous cell carcinoma; ctrl, control; DEPs, differentially expressed proteins.

TCGA data (Fig. 6B). Moreover, the expression of FBXO5 was significantly elevated in each pathological stage (Fig. 6C). In addition, the result of western blot analysis demonstrated that FBXO5 expression decreased significantly in a concentration-dependent manner after LCA treatment (Fig. 6D and E). Therefore, it was perceived that FBXO5 may be a potential target of LCA in the LSCC cells. Molecular docking has been widely used in prediction of the interactions between a target protein (enzyme) and drug molecules (ligands) at a molecular level (28). In the present study, the result revealed that LCA

is tightly bound to the active site of FBXO5 with a binding energy of -5.58 kcal/mol, in which the hydroxyl group of the LCA molecule forms three hydrogen bonds with the TYR52, CYS40 and GLY 39 (Fig. 6F and G). To identify the effect of FBXO5 in LSCC cells, H1703 cells were transfected with FBXO5 siRNA to knockdown the FBXO5. Si-FBXO5-2 was chosen for its significant inhibition on the expression of FBXO5 in H1703 cells (Fig. 6H). MTT experiment exhibited that the cell viability of H1703 cells treated with FBXO5-2 was lower compared with the negative control group (Fig. S1).

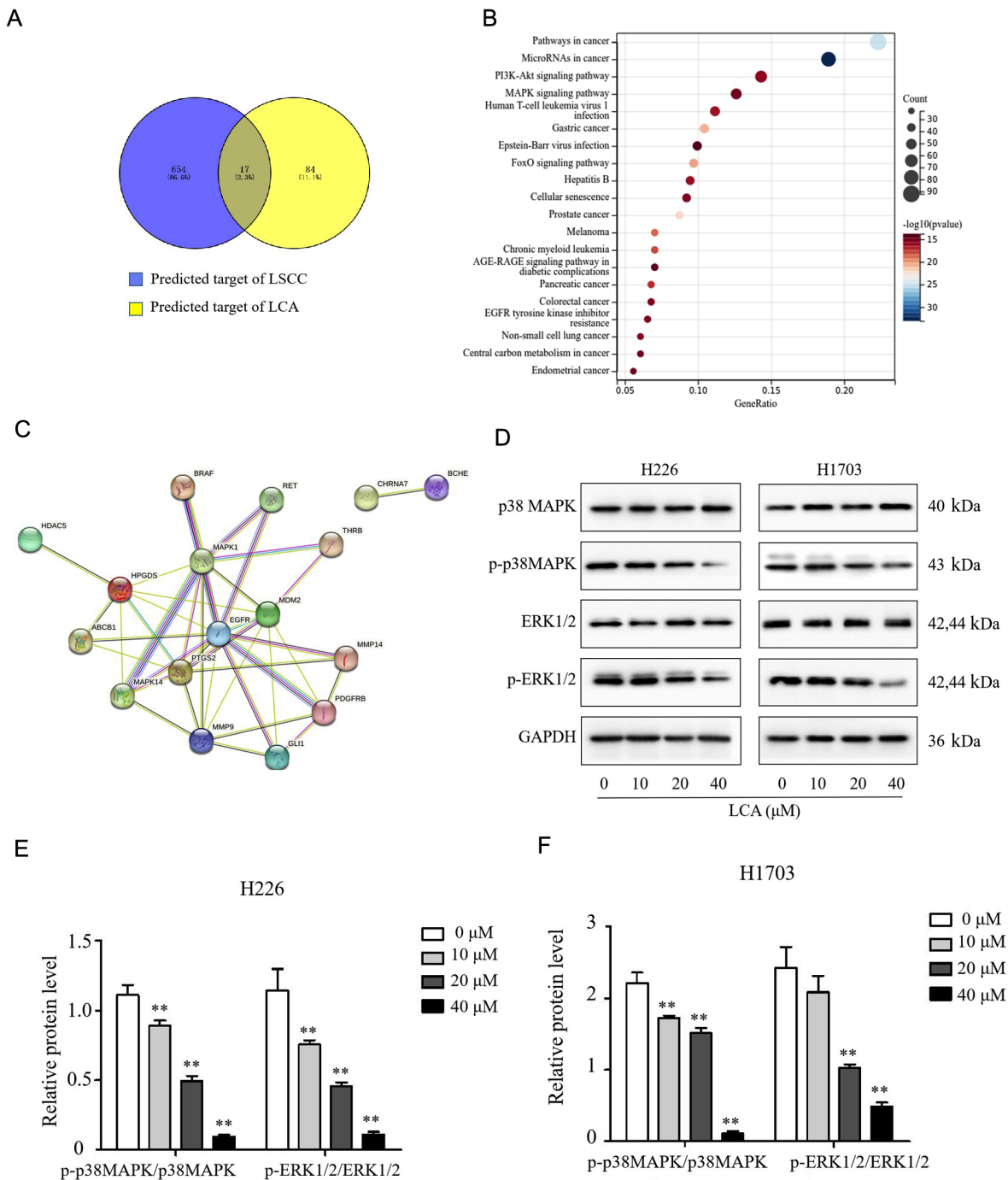


Figure 5. Network pharmacology analysis of the therapeutic target of LCA against LSCC. (A) Venn diagram revealed 17 overlapping genes for LCA target genes and LSCC-related genes. (B) The bubble chart illustrated enriched Kyoto Encyclopedia of Genes and Genomes pathways related to the therapeutic target. (C) Protein-protein interaction analysis revealed interaction of the 17 overlapping genes. (D-F) Western blot analysis results revealed the protein expression of p38 MAPK, p-p38 MAPK, ERK1/2 and p-ERK1/2 after treatment with LCA (0, 10, 20 and 40 μM) in LSCC cells. The experiments were repeated at least three times ($n=3$). ** $P<0.01$ vs. control. LCA, licochalcone A; LSCC, lung squamous cell carcinoma; p-, phosphorylated.

Moreover, FBXO5 silencing markedly reduced the expression levels of CDK2, CDK4, cyclin D1 and cyclin E (Fig. 6I). All the aforementioned results indicated that FBXO5 may be a potential target of LCA.

LCA inhibits the growth of LSCC in vivo. Tumor-transplanted mouse models of H1703 cells were used to evaluate the anti-tumor effect of LCA *in vivo*. As revealed in Fig. 7A, images of the mice and tumors of each group were captured. The maximum tumor volume was 1,418.48 mm^3 and the weight

was 0.9 g in the control group. Compared with control, the weights and volumes of the tumor in LCA treatment groups were significantly decreased (Fig. 7B and C). As shown in Fig. 7D, no significant changes in body weight were detected among groups. The body weight was decreased in the CDDP group compared with control, but the loss was not significant ($P>0.05$). In toxicological experiments, the changes of organ weight and histological changes are important indexes to evaluate the toxicity of drugs or compounds (29). To detect the possible potential toxicity to organs, the organ weight

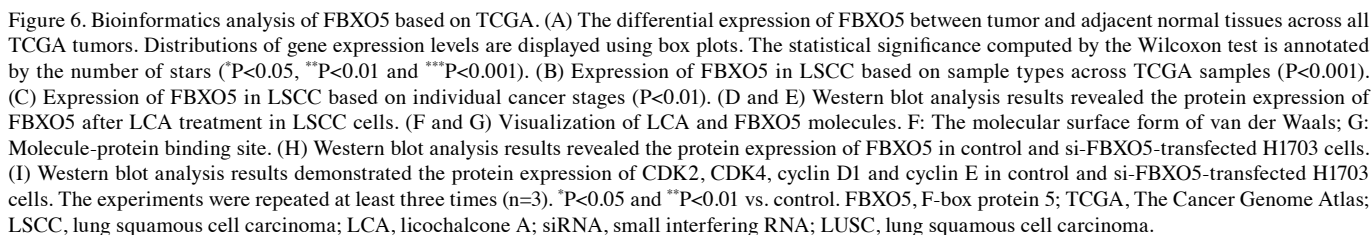


Table I. Top 10 differentially expressed proteins (LCA vs. Control).

Protein	Gene	LCA treatment vs. Control	
		Fold change	P-value
P01033	TIMP1	12.34	0.0016
Q96PD7	DGAT2	5.71	0.0045
P08138	NGFR	4.5617	0.0001
Q6ZNF0	ACP7	4.3918	0.0095
P00740	F9	4.3059	0.0013
Q6PCB0	VWA1	0.2497	0.0002
P15104	GLUL	0.2529	0.0012
Q6EMK4	VASN	0.2616	0.0376
Q8TDB6	DTX3L	0.2661	0.0011
Q9UKT4	FBXO5	0.2716	0.0146

LCA, licochalcone A.

was measured and histological examination was performed. No significant changes in organ weights were revealed among groups (Fig. 7E). H&E staining results revealed that no significant toxicities were observed in the vital organs of mice (Fig. 7F). Western blot analysis demonstrated that LCA treatment decreased the expression of FBXO5, p-ERK1/2 and p-p38MAPK (Fig. 7G and H) *in vivo*, which was consistent with the suppression effect of LCA on the MAPK pathway and the expression of FBXO5 *in vitro*. The aforementioned data indicated that LCA exhibited obvious antitumor activity with low toxicity on LSCC *in vivo*.

Discussion

Despite advancements in diagnosis and therapeutic techniques, the survival rates of lung cancer remain low in the world. LSCC is a highly heterogeneous malignancy with high tumor mutational burden. The molecular profile of LSCC was significantly different from that of adenocarcinoma (30,31). PD1/PD-L1 immune checkpoint blockade and targeted therapies improved the outcome of patients with lung adenocarcinoma, while these therapies were not available for patients with LSCC. Therefore, it is essential to find novel drugs or therapeutics which are effective and have low side effects. Previous studies demonstrated that Chinese traditional herbal medicine licorice displays anti-inflammatory, antitussive and antitumor activities (32-34). LCA is extracted from licorice and possess antitumor properties in several cancers (35-37).

In the present study, LCA effectively inhibited the proliferation of H226 and H1703 cells, while exhibiting no significant cytotoxicity against HBE cells even at a high concentration. The antitumor effect of LCA was also investigated via subcutaneous xenograft models and it was revealed that LCA suppressed xenograft tumor growth in mice. These results indicated that LCA effectively inhibited cell proliferation *in vitro* and xenograft tumor growth *in vivo*. Moreover, H&E

staining of vital organs indicated that the application of LCA was safe within a certain concentration range *in vivo*.

Cell cycle regulation is closely related to proliferation of tumors. Cell cycle is strictly regulated by cyclins and their associated specific CDKs (38), such as cyclin D1, CDK4, cyclin E and CDK2, which are of importance for the transition from G1 to S phase (39). In the present study, it was revealed that LCA increased the cell number in G1 phase in LSCC cells and decreased the protein levels of cyclin D1, cyclin E, CDK2 and CDK4. These findings were consistent with the previous studies that LCA induced G1 phase arrest in MCF-7 (14) and HCT-116 (40) cells. The aforementioned data suggested that LCA induced G1 phase arrest and downregulated the expression level of cell cycle-related protein.

Apoptosis is a programmed cellular process that occurs under either physiological or pathological conditions (41). Apoptosis exerts a vital role in the treatment of cancer, and induction of apoptosis is the eventual aim of numerous cancer therapies (42). The findings of the present study displayed that LCA induced apoptosis in LSCC cells and upregulated the level of cleaved caspase-3, cleaved PARP1 and Bax, meanwhile, LCA downregulated the level of Bcl-2. Therefore, LCA could induce cell apoptosis by the mitochondrial-mediated intrinsic pathway in LSCC cells. In the present study, the observed inhibition of cell viability and proliferation was not only dependent on increased cell apoptosis resulting from LCA treatment, but also in the cell cycle arrest. Apoptotic rates reflect part of proliferation inhibition.

Proteomics is widely used in drug development and cancer research (43). Proteomics combination with bioinformatics can analyze the mechanisms and biochemical processes of numerous complex diseases, such as diabetes and cancers (44). KEGG analyses of proteomic results revealed that the DEPs regulated by LCA were associated with the MAPK signaling pathway. And the network pharmacological analysis indicated that the MAPK1 (ERK2) and MAPK14 (p38 MAPK) were the core targets of LCA against LSCC. MAPK signaling pathways are involved in several biological processes and regulate cell proliferation, apoptosis and immune escape of several cancers (45). The ERK1/2 and p38 MAPK signaling pathways have been found to be activated and overexpressed in lung cancer (46,47). In the present study, LCA significantly suppressed ERK1/2 phosphorylation and p38 MAPK phosphorylation *in vivo* and *in vitro*.

Moreover, 4D-DIA proteomics also identified that FBXO5 protein expression was decreased after LCA treatment in LSCC cells. FBXO5 is vital in regulation of cycle proliferation and tumorigenesis. FBXO5 promotes cell proliferation and inhibits DNA re-replication via accumulation of cyclin A2 and geminin (48). FBXO5 was upregulated in various malignant tumors compared with matched normal tissues (25,49). A previous study has demonstrated that targeting FBXO5 could eliminate cutaneous squamous cell carcinoma cells with no effect on normal skin cells (50). Existing evidence has suggested that FBXO5 was upregulated in LSCC compared with normal tissue and associated with shorter OS in patients with LSCC (27). And FBXO5 may function as an oncogene and may be a novel therapeutic target in various malignancies (51). In the present study,

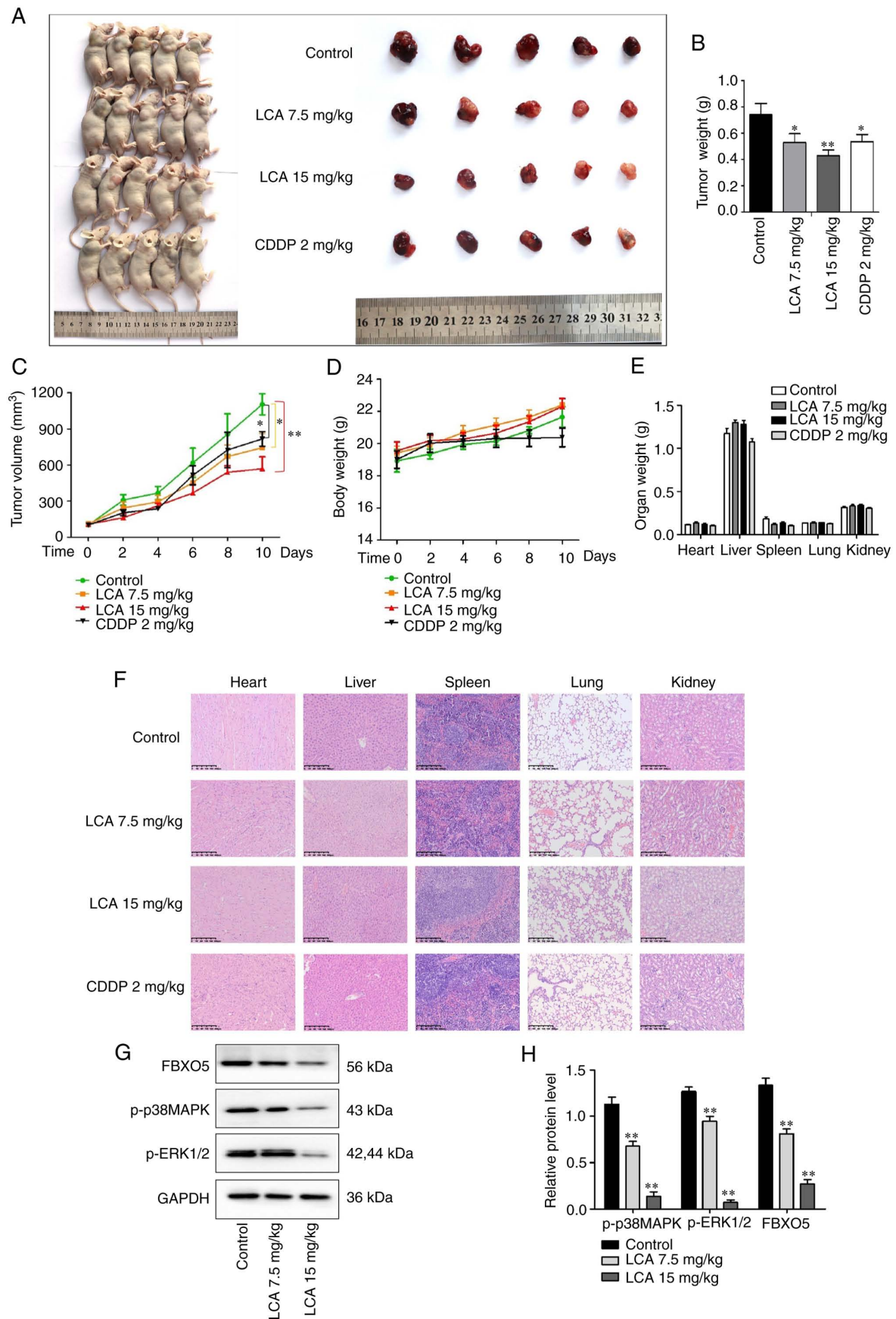


Figure 7. LCA suppresses lung squamous cell carcinoma xenograft tumor growth *in vivo* (n=5). (A) Representative images of xenograft tumor models and tumor tissues. (B) The wet weight of the mice xenograft tumors. (C) The tumor volumes of the mice xenograft tumors. (D) The body weight of the xenograft tumor mice. (E) The organ weight of the xenograft tumor mice. (F) The hematoxylin and eosin staining representative pictures of vital organs of the xenograft tumors mice (scale bar, 200 μ m). (G and H) The levels of FBXO5, p-p38 MAPK and p-ERK1/2 in tumor tissue determined by western blot analysis. The experiments were repeated at least three times (n=3). *P<0.05 and **P<0.01 vs. control. LCA, licochalcone A; FBXO5, F-box protein 5; CDDP, cisplatin; p-, phosphorylated. The body weight of the xenograft tumor mice.

compared with the adjacent normal tissue, FBXO5 was highly expressed in LSCC tissues based on the TCGA data, and FBXO5 level was significantly elevated in each pathological stage. The aforementioned results suggested that FBXO5 played an important role in LSCC and may be a therapeutic target for LSCC treatment. Western blot analysis revealed that LCA significantly decreased the FBXO5 protein expression. Furthermore, in order to ascertain the effect of FBXO5, MTT experiments were used to detect the cell viability in FBXO5-silenced H1703 cells. FBXO5 knockdown inhibited the cell viability and decreased the expression levels of CDK2, CDK4, cyclin D1 and cyclin E in H1703 cells. These findings indicated that FBXO5 protein knockdown inhibit the proliferation of H1703 cells.

There are certain limitations to the present study. In order to ascertain whether FBXO5 was the therapeutic target for antitumor effects of LCA, rescue experiments should be performed in the FBXO5-silenced H1703 cells in the future.

In summary, LCA inhibited the proliferation of LSCC cells, induced cell cycle arrest and apoptosis *in vitro* and significantly inhibited the tumorigenesis with few adverse effects *in vivo*. In addition, LCA inhibited ERK1/2 phosphorylation and p38 MAPK phosphorylation, and suppressed the expression of FBXO5 *in vivo* and *in vitro*. In conclusion, LCA may be a potential therapeutic candidate of LSCC.

Acknowledgements

Not applicable.

Funding

The present study was supported by the National Natural Science Foundation of China (grant no. 82160615).

Availability of data and materials

The datasets used and/or analyzed during the current study are available from the corresponding author on reasonable request.

Authors' contributions

XF, LW, JW and XD designed the experiments. XF and JW performed the experiments and data collection. XF wrote the original draft and revised the manuscript. GG and MJ analyzed the data. LW and JW critically reviewed and edited the manuscript. All authors read and approved the final version of the manuscript. XF and XD confirm the authenticity of all the raw data.

Ethics approval and consent to participate

The present study was approved by the Institutional Animal Care and Use Committee of Guilin Medical University (approval no. GLMC-IACUC-2021016; Guilin, China).

Patient consent for publication

Not applicable.

Competing interests

The authors declare that they have no competing interests.

References

1. Sung H, Ferlay J, Siegel RL, Laversanne M, Soerjomataram I, Jemal A and Bray F: Global cancer statistics 2020: GLOBOCAN estimates of incidence and mortality worldwide for 36 cancers in 185 countries. *CA Cancer J Clin* 71: 209-249, 2021.
2. Siegel RL, Miller KD and Jemal A: Cancer statistics, 2019. *CA Cancer J Clin* 69: 7-34, 2019.
3. Cheng TY, Cramb SM, Baade PD, Youlten DR, Nwogu C and Reid ME: The international epidemiology of lung cancer: Latest trends, disparities, and tumor characteristics. *J Thorac Oncol* 11: 1653-1671, 2016.
4. Herbst RS, Morgensztern D and Boshoff C: The biology and management of non-small cell lung cancer. *Nature* 553: 446-454, 2018.
5. Derman BA, Mileham KF, Bonomi PD, Batus M and Fidler MJ: Treatment of advanced squamous cell carcinoma of the lung: A review. *Transl Lung Cancer Res* 4: 524-532, 2015.
6. Rittmeyer A, Barlesi F, Waterkamp D, Park K, Ciardiello F, von Pawel J, Gadgeel SM, Hida T, Kowalski DM, Dols MC, *et al*: Atezolizumab versus docetaxel in patients with previously treated non-small-cell lung cancer (OAK): A phase 3, open-label, multicentre randomised controlled trial. *Lancet* 389: 255-265, 2017.
7. Gandara DR, Hammerman PS, Sos ML, Lara PN Jr and Hirsch FR: Squamous cell lung cancer: From tumor genomics to cancer therapeutics. *Clin Cancer Res* 21: 2236-2243, 2015.
8. Kennedy GT, Azari FS, Bernstein E, Nadeem B, Chang AE, Segil A, Sullivan N, Marfatia I, Din A, Desphande C, *et al*: A prostate-specific membrane antigen-targeted near-infrared conjugate for identifying pulmonary squamous cell carcinoma during resection. *Mol Cancer Ther* 21: 546-554, 2022.
9. Brahmer JR, Tykodi SS, Chow LQ, Hwu WJ, Topalian SL, Hwu P, Drake CG, Camacho LH, Kauh J, Odunsi K, *et al*: Safety and activity of anti-PD-L1 antibody in patients with advanced cancer. *N Engl J Med* 366: 2455-2465, 2012.
10. Topalian SL, Hodi FS, Brahmer JR, Gettinger SN, Smith DC, McDermott DF, Powderly JD, Carvajal RD, Sosman JA, Atkins MB, *et al*: Safety, activity, and immune correlates of anti-PD-1 antibody in cancer. *N Engl J Med* 366: 2443-2454, 2012.
11. Ferris RL, Blumenschein G Jr, Fayette J, Guigay J, Colevas AD, Licitra L, Harrington K, Kasper S, Vokes EE, Even C, *et al*: Nivolumab for recurrent squamous-cell carcinoma of the head and neck. *N Engl J Med* 375: 1856-1867, 2016.
12. Xia L, Liu Y and Wang Y: PD-1/PD-L1 blockade therapy in advanced non-small-cell lung cancer: Current status and future directions. *Oncologist* 24 (Suppl 1): S31-S41, 2019.
13. Wang ZF, Liu J, Yang YA and Zhu HL: A review: The anti-inflammatory, anticancer and antibacterial properties of four kinds of licorice flavonoids isolated from licorice. *Curr Med Chem* 27: 1997-2011, 2020.
14. Bortolotto LF, Barbosa FR, Silva G, Bitencourt TA, Belebony RO, Baek SJ, Marins M and Fachin AL: Cytotoxicity of trans-chalcone and licochalcone A against breast cancer cells is due to apoptosis induction and cell cycle arrest. *Biomed Pharmacother* 85: 425-433, 2017.
15. Lv H, Ren H, Wang L, Chen W and Ci X: Lico A enhances Nrf2-mediated defense mechanisms against t-BHP-induced oxidative stress and cell death via Akt and ERK activation in RAW 264.7 cells. *Oxid Med Cell Longev* 2015: 709845, 2015.
16. de Freitas KS, Squarisi IS, Aceso NO, Nicoletta HD, Ozelin SD, Reis Santos de Melo M, Guissone APP, Fernandes G, Silva LM, da Silva Filho AA and Tavares DC: Licochalcone A, a licorice flavonoid: Antioxidant, cytotoxic, genotoxic, and chemopreventive potential. *J Toxicol Environ Health A* 83: 673-686, 2020.
17. Hao W, Yuan X, Yu L, Gao C, Sun X, Wang D and Zheng Q: Licochalcone A-induced human gastric cancer BGC-823 cells apoptosis by regulating ROS-mediated MAPKs and PI3K/AKT signaling pathways. *Sci Rep* 5: 10336, 2015.
18. Li MT, Xie L, Jiang HM, Huang Q, Tong RS, Li X, Xie X and Liu HM: Role of licochalcone A in potential pharmacological therapy: A review. *Front Pharmacol* 13: 878776, 2022.

19. Lin M, Xu Y, Gao Y, Pan C, Zhu X and Wang ZW: Regulation of F-box proteins by noncoding RNAs in human cancers. *Cancer Lett* 466: 61-70, 2019.
20. Song Y, Lin M, Liu Y, Wang ZW and Zhu X: Emerging role of F-box proteins in the regulation of epithelial-mesenchymal transition and stem cells in human cancers. *Stem Cell Res Ther* 10: 124, 2019.
21. Reimann JD, Gardner BE, Margottin-Goguet F and Jackson PK: Emil regulates the anaphase-promoting complex by a different mechanism than Mad2 proteins. *Genes Dev* 15: 3278-3285, 2001.
22. Miller JJ, Summers MK, Hansen DV, Nachury MV, Lehman NL, Loktev A and Jackson PK: Emil stably binds and inhibits the anaphase-promoting complex/cyclosome as a pseudosubstrate inhibitor. *Genes Dev* 20: 2410-2420, 2006.
23. Di Fiore B and Pines J: Defining the role of Emil in the DNA replication-segregation cycle. *Chromosoma* 117: 333-338, 2008.
24. Vaidyanathan S, Cato K, Tang L, Pavey S, Haass NK, Gabrielli BG and Duijff PHG: In vivo overexpression of Emil promotes chromosome instability and tumorigenesis. *Oncogene* 35: 5446-5455, 2016.
25. Liu X, Wang H, Ma J, Xu J, Sheng C, Yang S, Sun L and Ni Q: The expression and prognosis of Emil and Skp2 in breast carcinoma: Associated with PI3K/Akt pathway and cell proliferation. *Med Oncol* 30: 735, 2013.
26. Guan C, Zhang J, Zhang J, Shi H and Ni R: Enhanced expression of early mitotic inhibitor-1 predicts a poor prognosis in esophageal squamous cell carcinoma patients. *Oncol Lett* 12: 114-120, 2016.
27. Wang K, Qu X, Liu S, Yang X, Bie F, Wang Y, Huang C and Du J: Identification of aberrantly expressed F-box proteins in squamous-cell lung carcinoma. *J Cancer Res Clin Oncol* 144: 1509-1521, 2018.
28. Pinzi L and Rastelli G: Molecular docking: Shifting paradigms in drug discovery. *Int J Mol Sci* 20: 4331, 2019.
29. Li F, Wang L, Cai Y, Luo Y and Shi X: Safety assessment of desaminotyrosine: Acute, subchronic oral toxicity, and its effects on intestinal microbiota in rats. *Toxicol Appl Pharmacol* 417: 115464, 2021.
30. Friedlaender A, Banna G, Malapelle U, Pisapia P and Addeo A: Next generation sequencing and genetic alterations in squamous cell lung carcinoma: Where are we today? *Front Oncol* 9: 166, 2019.
31. Cancer Genome Atlas Research Network: Comprehensive molecular profiling of lung adenocarcinoma. *Nature* 511: 543-550, 2014.
32. Hosseinzadeh H and Nassiri-Asl M: Pharmacological effects of *Glycyrrhiza* spp. and its bioactive constituents: Update and review. *Phytother Res* 29: 1868-1886, 2015.
33. Li K, Ji S, Song W, Kuang Y, Lin Y, Tang S, Cui Z, Qiao X, Yu S and Ye M: Glycybridins A-K, bioactive phenolic compounds from *Glycyrrhiza glabra*. *J Nat Prod* 80: 334-346, 2017.
34. Song W, Si L, Ji S, Wang H, Fang XM, Yu LY, Li RY, Liang LN, Zhou D and Ye M: Uralsaponins M-Y, antiviral triterpenoid saponins from the roots of *Glycyrrhiza uralensis*. *J Nat Prod* 77: 1632-1643, 2014.
35. Gao F, Li M, Yu X, Liu W, Zhou L and Li W: Licochalcone A inhibits EGFR signalling and translationally suppresses survivin expression in human cancer cells. *J Cell Mol Med* 25: 813-826, 2021.
36. Xu KD, Miao Y, Li P, Li PP, Liu J, Li J and Cao F: Licochalcone A inhibits cell growth through the downregulation of the Hippo pathway via PES1 in cholangiocarcinoma cells. *Environ Toxicol* 37: 564-573, 2022.
37. Hu C, Zuo Y, Liu J, Xu H, Liao W, Dang Y, Luo C, Tang L and Zhang H: Licochalcone A suppresses the proliferation of sarcoma HT-1080 cells, as a selective R132C mutant IDH1 inhibitor. *Bioorg Med Chem Lett* 30: 126825, 2020.
38. Mori M, Bogdan A, Balassa T, Csabai T and Szekeres-Bartho J: The decidua-the maternal bed embracing the embryo-maintains the pregnancy. *Semin Immunopathol* 38: 635-649, 2016.
39. Chang Z, Kuang HX, Zhou X, Zhu H, Zhang Y, Fu Y, Fu Q, Jiang B, Wang W, Jiang S, *et al*: Temporal changes in cyclinD-CDK4/CDK6 and cyclinE-CDK2 pathways: Implications for the mechanism of deficient decidualization in an immune-based mouse model of unexplained recurrent spontaneous abortion. *Mol Med* 28: 100, 2022.
40. Wu P, Yu T, Wu J and Chen J: Licochalcone a induces ROS-mediated apoptosis through TrxR1 inactivation in colorectal cancer cells. *Biomed Res Int* 2020: 5875074, 2020.
41. Morana O, Wood W and Gregory CD: The apoptosis paradox in cancer. *Int J Mol Sci* 23: 1328, 2022.
42. Khodavirdipour A, Piri M, Jabbari S, Keshavarzi S, Safaralizadeh R and Alikhani MY: Apoptosis detection methods in diagnosis of cancer and their potential role in treatment: Advantages and disadvantages: A review. *J Gastrointest Cancer* 52: 422-430, 2021.
43. Ji Q, Zhu F, Liu X, Li Q and Su SB: Recent advance in applications of proteomics technologies on traditional Chinese medicine research. *Evid Based Complement Alternat Med* 2015: 983139, 2015.
44. Monti C, Zilocchi M, Colugnat I and Alberio T: Proteomics turns functional. *J Proteomics* 198: 36-44, 2019.
45. Yong HY, Koh MS and Moon A: The p38 MAPK inhibitors for the treatment of inflammatory diseases and cancer. *Expert Opin Investig Drugs* 18: 1893-1905, 2009.
46. Greenberg AK, Basu S, Hu J, Yie TA, Tchou-Wong KM, Rom WN and Lee TC: Selective p38 activation in human non-small cell lung cancer. *Am J Respir Cell Mol Biol* 26: 558-564, 2002.
47. Sugiura R, Satoh R and Takasaki T: ERK: A double-edged sword in cancer. ERK-dependent apoptosis as a potential therapeutic strategy for cancer. *Cells* 10: 2509, 2021.
48. Marzio A, Puccini J, Kwon Y, Maverakis NK, Arbini A, Sung P, Bar-Sagi D and Pagano M: The F-box domain-dependent activity of EM11 regulates PARPi sensitivity in triple-negative breast cancers. *Mol Cell* 73: 224-237.e6, 2019.
49. Zhao Y, Tang Q, Ni R, Huang X, Wang Y, Lu C, Shen A, Wang Y, Li C, Yuan Q, *et al*: Early mitotic inhibitor-1, an anaphase-promoting complex/cyclosome inhibitor, can control tumor cell proliferation in hepatocellular carcinoma: Correlation with Skp2 stability and degradation of p27(Kip1). *Hum Pathol* 44: 365-373, 2013.
50. McHugh A, Fernandes K, Chinner N, Ibrahim AFM, Garg AK, Boag G, Hepburn LA, Proby CM, Leigh IM and Saville MK: The identification of potential therapeutic targets for cutaneous squamous cell carcinoma. *J Invest Dermatol* 140: 1154-1165.e5, 2020.
51. Liu P, Wang X, Pan L, Han B and He Z: Prognostic significance and immunological role of FBXO5 in human cancers: A systematic pan-cancer analysis. *Front Immunol* 13: 901784, 2022.



Copyright © 2023 Fan et al. This work is licensed under a Creative Commons Attribution-NonCommercial-NoDerivatives 4.0 International (CC BY-NC-ND 4.0) License.